J|A|C|S ARTICLES

Published on Web 04/22/2010

On the Origin of the Hydrophobic Water Gap: An X-ray Reflectivity and MD Simulation Study

Markus Mezger,*[,†,‡] Felix Sedlmeier,[¶] Dominik Horinek,*[,¶] Harald Reichert,[†,§] Diego Pontoni,[§] and Helmut Dosch[†,||]

Max-Planck-Institut für Metallforschung, Heisenbergstr. 3, 70569 Stuttgart, Germany, Department of Chemical Engineering, University of California, Berkeley, California 94720, Physik Department, Technische Universität München, 85748 Garching, Germany, and European Synchrotron Radiation Facility, 6 rue Jules Horowitz, 38043 Grenoble, France

Received December 16, 2009; E-mail: mmezger@lbl.gov; dominik.horinek@ph.tum.de

Abstract: The density deficit of water at hydrophobic interfaces, frequently called the hydrophobic gap, has been the subject of numerous experimental and theoretical studies in the past decade. Recent experiments give values for the interfacial depletion that consistently correspond to less than a monolayer of water. The main question which remained so far unanswered is its origin and the mechanisms affected by the chemistry and molecular geometry of a particular hydrophobic coating. In this work, we present a combined high-energy X-ray reflectivity and molecular dynamics simulation study of the water depletion at a perfluorinated hydrophobic interface with a spatial resolution on the molecular scale. A comparison of our experimental and computational results elucidates the underlying mechanisms that affect the extent of the interfacial depletion. The complex interplay between surface chemistry and topography precludes the existence of a direct and universal relation between the macroscopic contact angle and the nanoscopic water depletion.

Introduction

For decades, the interface between water and hydrophobic surfaces has caught the interest of chemists and physicists alike.[1,2] Structure and properties of this interface are intimately related to a proposed density depletion on the water side of the interface.[3] The existence of such a density depleted region at water−hydrophobic interfaces was confirmed by a variety of complementary numerical[4−8] and experimental techniques.[9,10] In the last years, the magnitude of the depletion as determined by X-ray or neutron scattering studies converged to the equivalent of a fraction of a water monolayer.[6,11−14] However, the origin of the observed depletion and its relation with macroscopic parameters such as the contact angle are still unclear.[15] So far, the vast majority of experimental and numerical studies used aliphatic hydrocarbons as generic hydrophobic model surfaces. To get a deeper understanding on how the interfacial water is affected by the molecular interaction with a hydrophobic substrate and its microscopic topography, it is essential to extend our focus to other materials.

In this study, we present high energy X-ray reflectivity[16] measurements and molecular dynamics (MD) simulations of the interface between water and a highly fluorinated self-assembled monolayer (SAM), shedding new light on these important questions. A comparison of this results with our previous work on hydrocarbon SAMs[11,12] reveals the influence of the different contributions to the observed interfacial depletion.

In molecular simulations of hydrophobic interfaces, the surface water interactions are freely variable parameters, whose systematic study gives insight into the mechanisms at play. When the interactions are chosen such that experimental systems are resembled, the depletion layer which is defined as the integrated normalized density deficit is of the order of about 2

[†] Max-Planck-Institut für Metallforschung.
[‡] University of California, Berkeley.
[¶] Technische Universität München.
[§] European Synchrotron Radiation Facility.
[||] Current address: Deutsches Elektronen Synchrotron, Notkestr. 85, 22607 Hamburg, Germany.

(1) Chandler, D. *Nature* **2002**, *417*, 491.
(2) Ball, P. *Nature* **2003**, *423*, 25–26.
(3) Chandler, D. *Nature* **2007**, *445*, 831–832.
(4) Lee, C. Y.; McCammon, J. A.; Rossky, P. J. *J. Chem. Phys.* **1984**, *80*, 4448–4455.
(5) Grigera, J. R.; Kalko, S. G.; Fischbarg, J. *Langmuir* **1996**, *12*, 154–158.
(6) Jensen, T. R.; Jensen, M. O.; Reitzel, N.; Balashev, K.; Peters, G. H.; Kjaer, K.; Bjornholm, T. *Phys. Rev. Lett.* **2003**, *90*, 086101.
(7) Giovambattista, N.; Rossky, P. J.; Debenedetti, P. G. *Phys. Rev. E* **2006**, *73*, 041604.
(8) Giovambattista, N.; Debenedetti, P. G.; Rossky, P. J. *J. Phys. Chem. B* **2007**, *111*, 9581–9587.
(9) Ge, Z.; Cahill, D. G.; Brown, P. V. *Phys. Rev. Lett.* **2006**, *96*, 186101.
(10) Subramanian, S.; Sampath, S. *J. Colloid Interface Sci.* **2007**, *313*, 64–71.
(11) Mezger, M.; Reichert, H.; Schöder, S.; Okasinski, J.; Schröder, H.; Dosch, H.; Palms, D.; Ralston, J.; Honkimäki, V. *Proc. Natl. Acad. Sci. U.S.A.* **2006**, *49*, 18401–18404.
(12) Mezger, M.; Schöder, S.; Reichert, H.; Schröder, H.; Okasinski, J.; Honkimäki, V.; Ralston, J.; Bilgram, J.; Roth, R.; Dosch, H. *J. Chem. Phys.* **2008**, *128*, 2447051−13.
(13) Poynor, A.; Hong, L.; Robinson, I. K.; Granick, S.; Zhang, Z.; Fenter, P. A. *Phys. Rev. Lett.* **2006**, *97*, 266101.
(14) Maccarini, M.; Steitz, R.; Himmelhaus, M.; Fick, J.; Tatur, S.; Wolff, M.; Grunze, M.; Janecek, J.; Netz, R. R. *Langmuir* **2007**, *23*, 598–608.
(15) Ocko, B. M.; Dhinojwala, A.; Daillant, J. *Phys. Rev. Lett.* **2008**, *101*, 039601.
(16) Reichert, H.; Honkimäki, V.; Snigirev, A.; Engemann, S.; Dosch, H. *Physica B (Amsterdam, Neth.)* **2003**, *336*, 46–55.

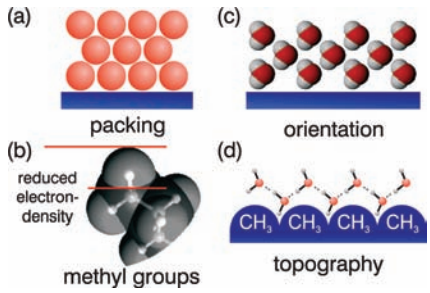

Figure 1. Sketch illustrating various structural features that could contribute to the observed density depletion at hydrophobic interfaces. The periodic arrangement should only indicate a tendency toward a certain structure rather than extended and stable long-range order. A detailed discussion is given in the text.

Å or less.[17−19] These values are similar or only slightly larger than what is experimentally observed. In experiments, there are only a limited number of distinct hydrophobic surface chemistries with the most common ones based on CH_3 terminated hydrocarbons. Another class of hydrophobic materials, that recently came to attention in liquid/liquid interfacial systems,[20] is composed of perfluorinated alkanes. Their investigation at a water/solid interfaces promises to give new insight into the phenomenon of water depletion.

On the molecular level, there are several structural features discussed that can contribute to a potential density depletion in the interfacial region (see Figure 1 for a summary of the main contributions). Packing effects in the liquid adjacent to a hard wall may lead to rearrangements in the liquid structure (Figure 1a). This was extensively studied by means of density functional theory of classical fluids, where the liquid is modeled as hard spheres with an attractive square well potential. One generic solution predicts an oscillatory profile in the liquid, typically extending a few molecular diameters into the bulk liquid.[21] It has been shown that for model parameters compatible with water the average density adjacent to a hydrophobic interface is reduced relative to its bulk value.[12] This effect is a universal feature, an intrinsic gap, that is common to all solid−liquid interfaces with comparable solid−liquid and liquid−liquid interactions.

Ocko et al.[15] recently discussed the contribution of volume effects in the terminal methyl groups of hydrophobic coatings to the interfacial density depletion (Figure 1b). Since the hydrogen atoms exhibit a very small electron density, they are essentially invisible to X-rays. However, they occupy some space at the interface. Studies of the bulk structure of crystalline paraffines[22] and the density profile of lipid bilayers[23] suggest that this contribution amounts to the equivalent of 31% of a water monolayer.

Molecular dynamics simulations,[4] Monte Carlo simulations,[19] and Sum Frequency Spectroscopy[24−28] indicate that the water molecules next to a hydrophobic interface are partially oriented. A so-called "ice-like" orientation is preferred, in which the outermost water molecules are oriented such that one hydrogen atom is preferentially pointing toward the solid surface (Figure 1c). As described by Ocko et al.,[15] this shifts the center of mass of the electron distribution of the water molecules away from the interface and results in a local, geometrically induced density depletion. On a laterally averaged mean-field level, these effects will not contribute to the integrated density depletion (see eq 1). However, in a real system, lateral corrugation is present and can lead to the described influence on the depletion length.

Finally, a real solid surface is never perfectly flat but exhibits at least atomic corrugation. The hydrogen bonding network in water may arrange more readily around interfacial protrusions than at a smooth solid wall (Figure 1d). Thus, the nanoscopic topography can influence the magnitude of the local density depletion. The characteristic length scales and curvatures[29,30] are given by the structural features of ice,[31] nonpolar solutes in liquid water[32] and fluctuations at the interface between liquid water and its vapor.[33] They are all in the same range and on the length scale of the corrugation of SAMs typically used to render a substrate hydrophobic.

In addition to these structural effects, density fluctuations of the liquid[34] result in a reduced contact density, which is most pronounced for very weak water-surface attractions. With increasing attraction of the liquid to the surface, this hydrophobic depletion d (see eq 1) gradually disappears. When the interaction strength of water molecules with an otherwise unchanged surface was varied, a linear relation between $1/d^2$ and θ was observed.[18] Because of the interplay between this contribution and the structural effects discussed before, different surface geometries lead to different slopes of the hydrophobic depletion versus contact angle curves.

Taking into account all these different contributions, the question arises how they add up to properties that are generally present at all hydrophobic surfaces and how much of the depletion is dependent on the specific molecular composition.

Experiments and Methods

For the high-energy X-ray reflectivity experiments, we have used Si wafers ((100) orientation, p-type boron-doped, resistivity 10−20 Ωcm, 625 μm thickness; Siltronics, Munich) covered with a native SiO_2 oxide layer and cut in pieces of 20 mm × 25 mm. Subsequently, the samples were solvent cleaned (isopropanol, acetone, chloroform) in an ultrasonic bath for 15 min each. To remove organic residues and prepare a hydrophilic hydroxyl terminated SiO_2 surface, the substrates were immersed in a freshly prepared piranha solution (one part H_2O_2 35% and three parts H_2SO_4 98%). After thorough rinsing in ultra pure water (Millipore

(17) Godawat, R.; Sumanth, N. J.; Garde, S. *Proc. Natl. Acad. Sci. U.S.A.* **2009**, 15119–15124.
(18) Sendner, C.; Horinek, D.; Bocquet, L.; Netz, R. R. *Langmuir* **2009**, *25*, 10768.
(19) Janecek, J.; Netz, R. R. *Langmuir* **2007**, *23*, 8417–8429.
(20) Kashimoto, K.; Yoon, J.; Hou, B.; Chen, C.; Lin, B.; Aratono, M.; Takiue, T.; Schlossman, M. L. *Phys. Rev. Lett.* **2008**, *101*, 076102.
(21) Evans, R.; Henderson, J. R.; Roth, R. *J. Chem. Phys.* **2004**, *121*, 12074–12084.
(22) Craievich, A. F.; Denicolo, I.; Douchet, J. *Phys. Rev. B* **1984**, *30*, 4782–4787.
(23) Wiener, M. C.; Suter, R. M.; Nagle, J. F. *Biophys. J.* **1989**, *55*, 315–325.
(24) Du, Q.; Freysz, E.; Shen, Y. R. *Science* **1994**, *264*, 826–828.
(25) Scatena, L. F.; Brown, M. G.; Richmond, G. L. *Science* **2001**, *292*, 908–912.
(26) Ye, S.; Nihonyanagi, S.; Uosaki, K. *Phys. Chem. Chem. Phys.* **2001**, *3*, 3463–3469.
(27) Shen, Y. R.; Ostroverkhov, V. *Chem. Rev.* **2006**, *106*, 1140–1154.
(28) Tian, C. S.; Shen, Y. R. *Proc. Natl. Acad. Sci. U.S.A.* **2009**, *106*, 15148–15153.
(29) Lum, K.; Chandler, D.; Weeks, J. D. *J. Phys. Chem. B* **1999**, *103*, 4570–4577.
(30) Schreiber, A.; Ketelsen, I.; Findenegg, G. H. *Phys. Chem. Chem. Phys.* **2001**, *3*, 1185–1195.
(31) Röttger, K.; Endriss, A.; Ihringer, J.; Doyle, S.; Kuhs, W. F. *Acta Crystallogr.* **1994**, *B50*, 644–648.
(32) Stillinger, F. H. *J. Solution Chem.* **1973**, *2*, 141–158.
(33) Sedlmeier, F.; Horinek, D.; Netz, R. R. *Phys. Rev. Lett.* **2009**, *103*, 136102.
(34) Mittal, J.; Hummer, G. *Proc. Natl. Acad. Sci. U.S.A.* **2008**, *105*, 20130.

Gradient), the platelets were blown dry in a stream of argon. Fluorinated SAMs were grafted on SiO_2 by chemical vapor surface modification following the route described by Hozumi et al.[35] The substrates were placed in a 700 mL desiccator together with a beaker containing 170 mg of 1*H*,1*H*,2*H*,2*H*-Perfluorodecyltrimethoxysilane (FAS17) (95%; ABCR, Karlsruhe). The desiccator was flushed with argon before heating to 110 °C for 16 h. To remove excess FAS17, the samples were rinsed in *n*-hexane and water prior to the transfer into the sample chamber.

X-ray Reflectivity Measurements. The experiments were performed using the HEMD instrument[16,36] at beamline ID15A of the European Synchrotron Radiation Facility (Grenoble, France) at an X-ray energy of 72.5 keV. Details on the experimental setup can be found in ref 12. The measurements cover scattering angles 2θ up to 1.4°, corresponding to a momentum transfer of 0.9 $Å^{-1}$ perpendicular to the interface. Thus, our experimental data carries real space information on a molecular length scale in the subnanometer regime. Interfacial electron density profiles were extracted from the experimental data sets by parameter refinement of a slab model (for details see ref 12).

Modeling. We have performed quantum chemistry calculations of a single $C_{10}H_5F_{17}$ molecule employing the Gaussian03 program.[37] The geometry was optimized on the HF/6-31G(3df) level of theory starting from an all anti conformation with the carbon backbone in a stretched configuration. The electron density was calculated on a 120 × 104 × 272 grid, and the electron density profile along the backbone of the chain was obtained by integration along the *x* and *z* directions.

Molecular dynamics simulations of $C_{10}H_5F_{17}$ and $C_{20}H_{42}$ SAMs were performed. For $C_{10}H_5F_{17}$, different geometries with different surface density and tilt angle were studied as shown in Table 2. The flexibility of the SAM is suppressed by freezing the SAM atoms in order to prevent tilting of the lesser dense SAMs. For the $C_{20}H_{42}$ SAM, a hexagonal lattice as described in Table 2 was used. In the computer simulations, the presence of the underlying substrate was ignored. The SAM models were brought in contact with SPC/E water and the contact angles and depletion layer thicknesses were calculated. All simulations were performed with Gromacs 3.3.[38] The thickness of the depletion layer *d* was calculated from the density deficit

$$d = \int_{-\infty}^{\infty} \mathrm{d}z \left[1 - \frac{\rho_1(z)}{\rho_1^0} - \frac{\rho_2(z)}{\rho_2^0} \right] \quad (1)$$

where $\rho_1(z)$ and $\rho_2(z)$ are the density profiles of the two phases at contact and ρ_1^0 and ρ_2^0 denote the respective bulk values. The contact angles were determined by the droplet approach.[39,40]

The influence of the molecular shape of the headgroup of both SAMs on the depletion length was determined by simulations of two SAMs in direct contact. For the fluorinated SAM, we have used the square-lattice model as described above. For comparison, we have performed the same simulation with the alkane SAM. The depletion length is then determined from the density profile as described above. An extensive description of the simulation methods and surface structures is given in the Supporting Information.

Results and Discussion

X-ray Reflectivity. Figure 2a shows the reflectivity of the dry FAS17 coated substrate. The observed pattern qualitatively agrees with the reflectivity reported by Geer et al. for similar fluorinated SAMs.[41] The oscillatory structure factor R/R_F (see inset of Figure 2) with minima around 0.21 and 0.72 $Å^{-1}$ suggests a real space electron density profile governed by a layer of approximately $2\pi/\Delta q = 12.3$ Å thickness. The high reflectance relative to the Fresnel curve (green curve) indicates a small surface roughness on the level of the molecular corrugation. Compared to SAMs with long hydrocarbon chains, for example, OTS (octadecyl-trichlorosilane) on silicon, exhibiting pronounced interference fringes with intensity modulations over more than 2 orders of magnitude,[12,42] the FAS17 reflectivity shows only weak modulations. This is a direct consequence of the less balanced contrast ratio at the SAM/vacuum and SAM/substrate interface caused by the much higher electron density of the fluorine in FAS17 compared to the hydrogen atoms in OTS.[43]

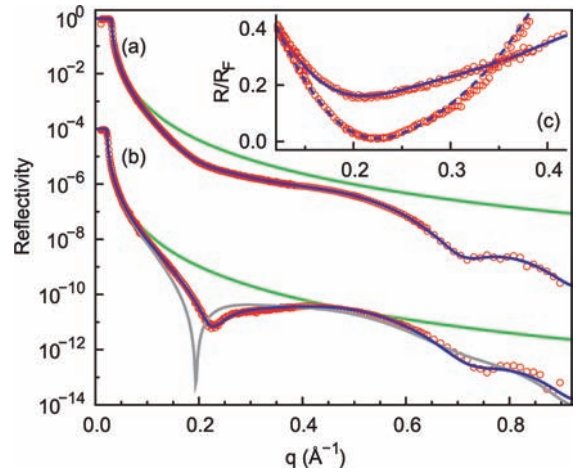

Figure 2. X-ray reflectivity (red circles) from a FAS17 SAM grafted on SiO_2 terminated silicon wafers in air (a) and with the sample immersed in degassed water (b). For reference, the green lines give the Fresnel reflectivity R_F of an ideal silicon substrate. Blue lines are best fits to the experimental data (see text). The gray line represents the calculated reflectivity using the unmodified SAM parameters from the dry measurements without an interfacial water layer. (c) The inset shows a magnification of the structure factor R/R_F for the dry (solid line) and the water-immersed sample (dashed line).

By parameter refinement of a slab model (blue curve in Figure 2a), we were able to reproduce the reflectivity of the dry FAS17 surface perfectly. The electron density profile (red curve in Figure 3) includes the semi-infinite silicon substrate for which literature values were used and a native SiO_2 layer. The FAS17 SAM is modeled by a partially cross-linked silane anchor group with the assumed stoichiometry SiO_2H, an interconnecting hydrocarbon chain C_2H_4 and the perfluorinated tail C_8F_{17}. To take into account the known structure of the FAS17 molecule, the mass ratio of its three parts (layers 3−5 in Table 1) were constrained by their molecular compositions. The length of the fluorocarbon chain was fixed to the all trans length of 10.4 Å for a CF_3-$(CF_2)_7$ chain as derived from quantum chemical calculations (green curve in Figure 3). This corresponds to a perpendicular alignment of the perfluorinated tail as suggested

(35) Hozumi, A.; Ushiyama, K.; Sugimura, H.; Takai, O. *Langmuir* **1999**, *15*, 7600–7604.
(36) Honkimäki, V.; Reichert, H.; Okasinski, J. S.; Dosch, H. *J. Synchrotron Radiat.* **2006**, *13*, 426–431.
(37) Frisch, M. J. et al. *Gaussian 03*, Revision C.01, Gaussian, Inc., Wallingford, CT, 2004.
(38) Lindahl, E.; Hess, B.; van der Spoel, D. *J. Mol. Model.* **2001**, *7*, 306.
(39) Werder, T.; Walther, J. H.; Jaffe, R. L.; Halicioglu, T.; Koumoutsakos, P. *J. Phys. Chem. B* **2003**, *107*, 1345.
(40) Sedlmeier, F.; Janecek, J.; Sendner, C.; Bocquet, L.; Netz, R. R.; Horinek, D. *Biointerphases* **2008**, *3*, FC23.
(41) Geer, R. E.; Stenger, D. A.; Chen, M. S.; Calvert, J. M.; Shashidhar, R. *Langmuir* **1994**, *10*, 1171–1176.
(42) Tidswell, I. M.; Rabedeau, T. A.; Pershan, P. S.; Kosowsky, S. D.; Folkers, J. P.; Whitesides, G. M. *J. Chem. Phys.* **1991**, *95*, 2854–2861.
(43) Wasserman, S. R.; Whitesides, G. M.; Tidswell, I. M.; Ocko, B. M.; Pershan, P. S.; Axe, J. D. *J. Am. Chem. Soc.* **1989**, *111*, 5852–5861.

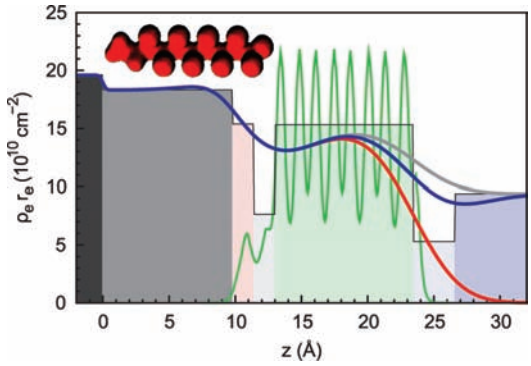

Figure 3. Electron density profiles of the dry FAS17 SAM on a Si/SiO_2 substrate (red curve) and the sample immersed in water with (blue curve) and without (gray curve) an interfacial water layer of reduced density. The profiles were extracted from the X-ray reflectivity data by parameter refinement of a slab model (boxes) including interfacial roughness and resonant scattering corrections for 72.5 keV X-rays. The green curve shows the laterally averaged electron density distribution of $CH_3CH_2(CF_2)_7CF_3$ as obtained from quantum chemistry calculations. In the upper left corner its van der Waals surface is shown.

Table 1. Parameters for FAS17 SAMs on a Si/SiO_2 Substrate Obtained from Parameter Refinement of a Slab Model with Layer Thickness *l*, Mass Density ρ, and Interfacial Roughness σ[a]

no.	layer		*l* [Å]	ρ [g cm^{-3}]	σ [Å]
5	perfluorinated tail	C_8F_{17}	10.4*	1.88†	2.8
4	hydrocarbon chain	C_2H_4	1.7	0.79†	4.0*
3	silane anchor	SiO_2H	1.6	1.79†	2.2
2	native SiO_2	SiO_2	9.8	2.16	1.4
1	silicon bulk	Si	–	2.32*	0.2*

[a] Parameters that were fixed are marked with asterisk (*). The density ratios of the layers associated with the different subunits of FAS17 (marked with a †) were constrained by the molecular composition of an anchored SAM.

by Zuo and co-workers.[44] The refractive index of each slab was calculated using the NIST scattering database.[45]

Table 1 summarizes the fitting parameters. Dense packing of the SAMs is confirmed by a 12% higher mass density of the fluorinated tail compared to perfluorohexan with 1.68 g cm^{-3}. This implies an area of 35.6 Å^2 per fluorocarbon chain corresponding to a diameter of 6.0 Å in a square lattice. This is in good agreement with an area of ~32 Å^2 determined from Langmuir isotherms of a monolayer of l*H*,l*H*,2*H*,2*H*-perfluorododecyltriethoxysilane on water.[46] The surface roughness of 2.8 Å is determined by the intrinsic corrugation of the terminal CF_3 groups, the inhomogeneities in the SAM, and the additional roughness imposed by the underlying SiO_2 substrate. Figure 3 also shows that the interconnecting hydrocarbon part and the silane anchor group are strongly smeared out and cannot be distinguished as independent slabs. The total thickness of 13.7 Å for the FAS17 SAM layer confirms the qualitative estimate of 12.3 Å deduced from the features in the reflectivity curves and is in good agreement with the 14.1 Å found for a similar perfluorinated SAM.[47] More details on the modeling and parameter refinement can be found in the Supporting Information.

Table 2. Compilation of Depletion Lengths *d* and Contact angles θ Extracted from X-ray Reflectivity (XRR) Measurements and MD Simulations Together with Literature Data[a]

system			*A* [Å^2]	ρ [g/cm^3]	α	*d* [Å]	θ
FAS17		XRR	35.6	1.88	0°	1.38	112° [46]
FAS17	sq	MD	31.4	2.11	0°	1.42	142°
FAS17	sq	MD	36.0	1.84	0°	1.34	144°
FAS17	sq	MD	44.9	1.82	35.77°	1.00	142°
FAS17	hex	MD	44.9	1.82	35.77°	1.20	137°
OTS[12]		XRR	23	0.86	20°	1.1	112° [43]
OTS	hex	MD	25.0	0.86	30°	1.4	135°
paraffine[6]		XRR	n.a.	1.03	n.a.	1.0	112°

[a] For the computer simulations, square (sq) or hexagonal (hex) packing was used to model the SAMs. The hydrophobic chains occupy an area *A*, have a mass density ρ, and are tilted by an angle α with respect to the substrate normal. For comparison, the mass densities of liquid perfluorohexane and semi crystalline PTFE are 1.68 and 2.16 g/cm^3.

Figure 2b shows the reflectivity recorded from the same FAS17 sample immersed in degassed water (red circles). The most prominent feature is the appearance of a pronounced dip at 0.21 Å^{-1} where the signal decays more than 2 orders of magnitude below the Fresnel reflectivity before recovering again around 0.5 Å^{-1}. This indicates a density profile with the contrast ratio between the water-SAM and SAM-silicon interface close to unity allowing for close to perfect destructive interference of the reflected waves.

Employing the parameters obtained for the dry FAS17 SAM (see Table 1), we can now calculate the X-ray reflectivity of the sample immersed in water assuming that the water is in direct contact with the SAM without any changes in density at the interface (Figure 2b, gray curve). Significant differences to the experimental curve lead to the conclusion that major rearrangements in the interfacial water structure adjacent to the hydrophobic substrate are present. They lead to a local deviation of the laterally averaged electron density from its bulk value. To account for this, we extended the model profile by an interfacial water layer of variable density. For an integrated density deficit $d(\rho - \rho_{H_2O})$ of 1.4 Å g cm^{-3} distributed over 3.2 Å, the calculated reflectivity (blue curve in Figure 2b) matches the experimental data almost perfectly. This value corresponds to 49% of a water monolayer missing at the interface We note here that the experimental value for the density deficit determined for a hydrocarbon (OTS) SAM with exactly the same experimental setup is 39%.[11,12]

Computer Modeling. The van der Waals surface of a single $CH_3CH_2(CF_2)_7CF_3$ molecule is shown in the inset of Figure 3. While the electron density of the CH_3 end group (left side) is almost isotropic, the fluorinated part (right side) exhibits distinct protrusions originating from the larger and electron richer fluorine atoms.

Table 2 shows the depletion length *d* and contact angle θ obtained from molecular dynamics simulations of water on different FAS17 SAM models (for details see eq 1). The predicted contact angles range from 137° for a hexagonally arranged grid of tilted chains to 144° for a square grid of untilted chains. The depletion length predicted from these models is between 1.0 and 1.4 Å. The depletion length is smallest for the two model SAMs with tilted chains. The contact angle range compares well to results of Li et al.,[48] who observed a contact angle of 138° for $C_{10}H_5F_{17}$ in a square grid arrangement. We

(44) Zuo, J.; Keil, P.; Valtiner, M.; Thissen, P.; Grundmeier, G. *Surf. Sci.* **2008**, *602*, 3750–3759.
(45) Chantler, C. T. *J. Phys. Chem. Ref. Data* **2000**, *29*, 597–1048.
(46) Paso, K.; Helberg, R. M. L.; Raaen, S.; Sjöblom, J. *J. Colloid Interface Sci.* **2008**, *325*, 228–235.
(47) Tidswell, I. M.; Ocko, B. M.; Pershan, P. S.; Wasserman, S. R.; Whitesides, G. M.; Axe, J. D. *Phys. Rev. B* **1990**, *41*, 1111–1128.
(48) Li, X.; Li, J.; Eleftheriou, M.; Zhou, R. *J. Am. Chem. Soc.* **2006**, *128*, 12439.

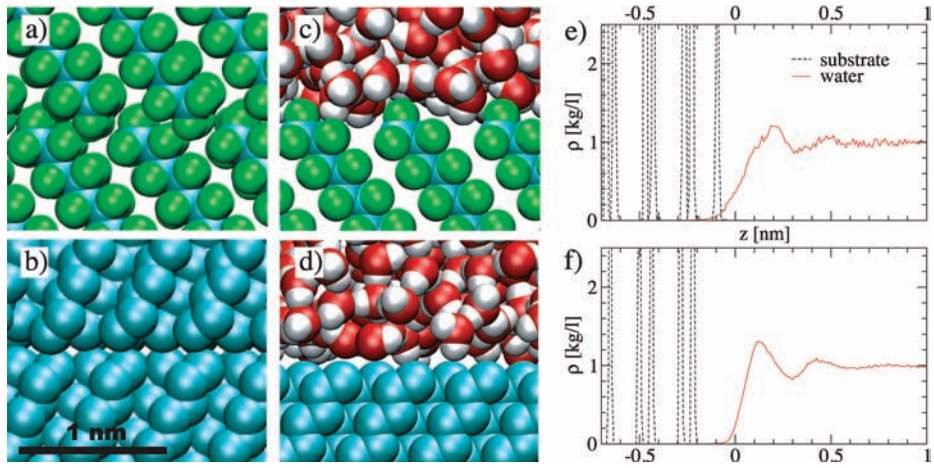

Figure 4. (a and b) Snapshots of a simulation of two SAMs in direct contact, and (c and d) in contact with water. (a and c) Fluorinated SAMs; (b and d) alkane SAMs. (e and f) Mass density profile of the water (full lines) and the substrates (dashed lines) as obtained from the MD simulations for the fluorinated SAM (square lattice) (e) and the alkane SAM (f). The density of the substrate shows a delta-peak like profile, since the substrate is frozen during the simulations. The origin of the *z*-axis is placed at the Gibbs dividing surface of the water density.

note here that the contact angle in the simulations is systematically larger than observed in experiments owing to three effects: (i) The simulations neglect attractive long-range van der Waals forces beyond the applied cutoff radius. (ii) The presence of the silicon substrate, which was ignored in the simulations, causes a further reduction of the contact angle.[49] The thinner the film the stronger this effect will be. (iii) The line tension of the nano scale water droplet used in the simulations increases the contact angle, but is irrelevant for a macroscopic water droplet.

For a simplified hydrocarbon SAM with square lattice geometry, $\theta = 126°$ and $d = 2.1$ Å were obtained.[19] A similar, hexagonally arranged hydrocarbon SAM with the same bulk density gave a contact angle of $\theta = 118°$ and $d = 2.0$ Å. Our own simulations of a hexagonal alkane SAM with a slightly different geometry yield a contact angle of $\theta = 135° \pm 4°$ and a depletion of $d = 1.4$ Å. In our OTS model, the chains are tilted by 30°, whereas the models of ref 19 assume no tilt. Consistent with the FAS17 results, the tilted model predicts a slightly smaller depletion length.

The polarity of a C−F bond is opposite to the polarity of a C−H bond, and the different depletion could originate from a response of the water orientation to the resulting inverted electrostatic potential (see Figure 1c). However, simulations in which this polarity is completely ignored give essentially unchanged results for the depletion layer. Therefore, a relation between the inverted polarity and the depletion layer can be ruled out.

In Figure 4a,b, we show snapshots of the contact region when two identical SAMs are in contact in the absence of water. Because of the shape of the CF_3 head groups, the fluorinated SAMs can interpenetrate each other (Figure 4a), which leads to a vanishing depletion length. In contrast, the CH_3 head groups are spherical and no interpenetration is observed for the alkane SAMs (Figure 4b), resulting in a depletion length of 1.2 Å.

Conclusions

For a comprehensive interpretation of the results, we summarize our five distinct observations:

(i) The experimental value for the water gap obtained at the FAS17 interface amounts to 49% of a water monolayer (this work) compared to 39% at an OTS interface.[11] High-energy X-rays cannot distinguish between electrons that belong to the SAM (contribution to ρ_1) and electrons that belong to the water (contribution to ρ_2). They only sense the combined, total electron density profile and provide no information on how the interfacial depletion is distributed. Thus, for comparison of the depletion length d extracted from MD simulations via eq 1 with the experimental values, we have to make the assumption that the gap is either caused entirely by the aqueous phase, the SAM, or by a combination of both. Assuming a pure water gap, we obtain a depletion length of 1.4 Å for FAS17 and 1.1 Å for OTS versus 2.1 and 0.9 Å for a contribution from the SAMs only. In both cases, the depletion obtained in MD simulations is in good agreement with the experimental values assuming the depletion layer to be caused primarily by the interfacial water.

(ii) The experimental contact angle of water is approximately 112° on both OTS and FAS17.[35,43,44,46] From molecular dynamics simulations, we obtain a contact angle of water on fluorinated SAMs in the range of 137−144°. These values are significantly larger than the contact angle on a hydrocarbon SAM, which is 135° in our own simulations, whereas a previous study found 126° and 118° for two model hydrocarbon SAMs.[19] Long-ranged interactions with the SiO_2 substrate,[50] which are neglected in the simulations, reduce the contact angle for both the FAS and OTS SAM. This reduction is more pronounced for the much shorter FAS17 SAMs than for OTS, and resulting water contact angles are similar on both SAMs.

(iii) Molecular dynamics simulations of the interface of hydrophobic SAMs with water yield a depletion length between 1.0 and 1.4 Å for different FAS17 models and 1.4 Å for OTS.

(iv) A detailed analysis, which is presented in the Supporting Information, shows that the orientational distributions of the interfacial water molecules adjacent to the FAS17 and OTS interfaces are comparable, and not affected by the inverted polarity of a CF versus a CH bond. The simulations show a broad orientational distribution with the hydrogen atoms pointing

(49) Seemann, R.; Herminghaus, S.; Jacobs, K. *Phys. Rev. Lett.* **2001**, *86*, 5534.

(50) Fetzer, R.; Jacobs, K.; Münch, A.; Wagner, B.; Witelski, T. P. *Phys. Rev. Lett.* **2005**, *95*, 127801.

preferentially toward the substrate which is in agreement with earlier MD simulations.[4,40] Spectroscopy experiments[24,28] observed a signature similar to the one found for ice and attributed it to an enhanced ordering of the water molecules adjacent to a hydrophobic solid−liquid interface. However, this does not prove the presence of a stable "ice-like" layer and the commonly accepted view is that the observed orientations are originating from the average of a wildly fluctuating liquid interface rather than a well-ordered, solid-like layer.[51] Therefore, the contribution from the interfacial water orientation to the density depletion would be less than the upper limit of approximately 1 Å assuming a well-ordered layer.[15]

(v) Simulation results show that the depletion length between slabs of perfluorinated alkyl chains in direct contact is vanishing. In contrast, a depletion length of 1.2 Å is found in between hydrocarbon SAMs. This value is slightly smaller than the 1.8 Å calculated from the structure of bulk crystalline alkanes.[15,22]

The simulations where two SAMs are brought in direct contact with each other give an estimate of the contribution to the interfacial depletion that is solely caused by the end groups. The different behavior of the hydrocarbon and perfluorinated tails originates primarily from the interdigitation of the chains. Of course, the liquid/SAM interfaces behave rather differently since the smaller and more mobile water molecules can occupy vacant space much more readily. However, the resulting depletion serves as an upper estimate of the magnitude of simple topography and excluded volume effects of the terminal methyl versus trifluoromethyl groups.

A more in-depth understanding of these phenomena can be achieved by considering the relevant length scales in our system. Our X-ray reflectivity measurements give an area of 23 and 35.6 Å^2 per OTS and FAS17 molecule, respectively. This is in good agreement with the size of the terminal caps of the SAMs as estimated from the molecular geometry of methane that is almost spherical with a diameter of 4.2 Å[52] and the larger tetrafluoromethane showing distinct protrusions in its molecular surface.[53] Likewise, linear alkyl chains in all-trans configuration are almost cylindrical objects while their perfluorinated analogues exhibit a more complex structure as supported by our quantum chemistry calculations shown in the inset of Figure 3. The characteristic length scales of the water interface are related to its capillary wave spectrum. Simulations show that the free water interface displays a crossover from bending to tension at 0.5 Å in lateral direction to the surface, and has an intrinsic roughness of up to 8 Å, which is due to the reconstruction of the hydrogen bonding network.[33] Since the dimensions of the water structure and the SAMs appear on the same length scale, the organization of the hydrogen bond network and thus the interfacial depletion will depend on the topography of the interface (see Figure 1d).

In our experiments, we are limited to one data point per chemically distinct surface. However, by comparing the experimental result with molecular dynamics simulations where the arrangements of the hydrophobic SAMs vary systematically, we gain information on the topographic contribution to the interfacial density depletion. Table 2 shows that a less-pronounced hydrophobic surface character as quantified by the water contact angle does not necessarily coincide with a decreased depletion length. Calculations for different lattice geometries, inclination angles, and packing densities in the physically relevant parameter range show that the depletion length at the same molecular surface can vary by up to 40% without any systematic link to the contact angle.

Our findings are not in conflict with previous MD simulations where hydroxyl groups were gradually added to a hydrophobic surface composed of densely packed alkyl chains,[19] since the underlying forces are different in the case of polar head groups. In accordance to our results, changes in a structural property, in this case the inclination angle of the hydroxyl groups did not result in a monotonic relation between the wetting coefficient and the interfacial depletion. A recent simulation study, where the depletion widths of SAMs with different head groups were analyzed,[17] supports our view. Even if the definition of the depletion width in this work does not correspond to the depletion measured in X-ray reflectivity experiments, the observation is similar: the influence of the specific headgroup chemistry on the depletion, in particular in the case of CF_3 and CH_3 end groups, cannot be explained merely by the contact angle of the respective SAM. Only for polar head groups a slight tendency toward smaller density depletions was found.

In the following, we discuss our observations along the lines of a recent simulation study of corrugated H-terminated diamond surfaces.[18] For a surface of given corrugation, a variation of the Lennard−Jones interaction strength revealed that $1/d^2$ scales linearly with the contact angle θ and the slope is characteristic for the molecular-scale surface roughness. The smallest depletion was always observed for the most corrugated surface, whether the values were plotted as a function of the Lennard−Jones interaction parameters, or the resulting contact angle. This shows that the density fluctuations at the interface are entangled with the surface topography, because the fluctuations of the water interface have a nontrivial length dependence.[33] For all studied surface corrugations, realistic water-surface interactions predict that the depletion length is less than 2 Å. In this study, we are dealing with a chemically rather different surface material, self-assembled oligomer monolayers as compared to crystalline diamond. Nevertheless, our results agree well with the study of diamond surfaces.

In conclusion, atomistic simulation studies of realistic molecularly packed surfaces and X-ray reflectivity measurements of hydrocarbon and perfluorinated SAMs give consistent values for depletion layer thicknesses of at most 2.1 Å. The depletion layer is influenced by a complex interplay between the chemistry and the topographic properties of each specific hydrophobic surface. Because the density fluctuations are entangled with the surface topography, there is no clear-cut distinction between hydrophobic and nonhydrophobic contributions to the magnitude and extent of the water gap and it is not possible to obtain a general simple rule to calculate the interfacial depletion from macroscopic quantities such as the contact angle. However, by comparison of the results from MD simulations and X-ray reflectivity for two hydrophobic model interfaces, we found typical values that can serve as estimates for the interpretation of observations on more complex interfaces, for which consistent experimental and computational data is not available.

On hydrocarbon interfaces, terminal methyl groups lead to a depletion of the electron density near the surface. In X-ray scattering experiments, this contribution cannot be separated from changes in the water density. Our simulations of two hydrocarbon SAMs in contact gave an upper estimate of 0.6 Å (i.e., half of the depletion length of 1.2 Å observed in the alkane SAM simulation) for this apparent water depletion, that is,

(51) Ball, P. *Chem. Rev.* **2008**, *108*, 74.
(52) Mack, E. *J. Am. Chem. Soc.* **1932**, *54*, 2141–2165.
(53) Bol'Shutkin, D. N.; Gasan, V. M.; Prokhvatilov, A. I.; Erenburg, A. I. *Acta Crystallogr.* **1972**, *B28*, 3542–3547.

significantly smaller than the values for the OTS−water interface. The water depletion on FAS17, for which no such end-group effects are present, is comparable in size. Thus, the contribution from terminal methyl groups cannot solely explain the observed density depletion. While calculations for well ordered, "ice-like" interfacial structures give an upper estimate of about 1 Å for the contribution from interfacial water orientation, the broad distributions found in the MD simulations suggest that the share from a strongly fluctuating fluid adjacent to a hydrophobic solid is significantly smaller. In particular, our MD simulations showed that the molecular water orientation is not influenced by the different polarity of the CH_3 and CF_3 head groups. The comparison of different molecular arrangements of the SAMs suggests that the surface morphology strongly affects the interfacial depletion and can be related in a counterintuitive way to the contact angle, commonly used as a macroscopic measure to quantify hydrophobicity. This is of particular importance for more complex soft and biological surfaces that generally tend to show strong corrugations on the length scale of a few angstroms. In addition, there are contributions from molecular packing and capillary wave-like fluctuations that are generic to all fluid interfaces. For smooth interfaces, all these different parts add up to typically less than the equivalent of a molecular monolayer of water, that is, 2.8 Å, missing at the solid/liquid interface. Significantly stronger depletion effects can only be expected for super hydrophobic surfaces with larger-scale patterns that need to be engineered rather than chemically synthesized.

Acknowledgment. The authors thank Benjamin M. Ocko (Brookhaven National Laboratory) and Roland R. Netz (Technische Universität München) for helpful discussions, V. Honkimäki, S. Schöder, J. Okasinski (ESRF, Grenoble) for assistance with the synchrotron experiments at ID15A, and P. Dreier (Siltronic AG, Munich) for supplying the high quality silicon wafers. D.H. thanks the Leibniz Rechenzentrum for supercomputing access and the Nanosystems Initiative Munich (NIM) for financial support. F.S. is supported by the Elitenetzwerk Bayern in the framework of the doctorate program Materials Science of Complex Interfaces.

Supporting Information Available: Details on the analysis of the experimental data, the molecular dynamics simulations and complete ref 37. This material is available free of charge via the Internet at http://pubs.acs.org.

JA910624J